PDE Constrained Optimization Applied to Plate Motions and Mantle Flow

Vishagan Ratnaswamy[1,2], Michael Gurnis[2], Georg Stadler[3], Laura Alisic[2,4], Omar Ghattas[3]

1. Graduate Aerospace Laboratories (GALCIT), California Institute of Technology, 1200 E. California Blvd, Pasadena, CA, 91125
2. Seismological Laboratory, California Institute of Technology, 1200 E. California Blvd, Pasadena, CA 91125
3. Institute for Computational Engineering and Sciences, The University of Texas, Austin, TX 78712
4. Now at: Bullard Laboratories, University of Cambridge, Cambridge, UK

Introduction

Numerical studies of plate tectonics have previously suffered from poor resolution until recent models using Adaptive Mesh Refinement (AMR) in *Stadler et. al (2010)*, and *Alisic et al. (2012)*. While the studies provided resolution as fine as 1km at plate boundaries, a more accurate model can be attained by using inverse methods that are applied to the equations that govern mantle convection.

Mathematical Development

The inverse problem is given as follows where we seek to minimize the misfit in surface velocities given in (1), where Γ is the prefactor of contained in the rheological law we are using.

$$\min_{\Gamma} J = \int_{\partial S} |u - u_{true}|^2 ds \qquad (1)$$

Subject to the PDE constraints given in (2) with free slip boundary conditions.

$$\nabla \cdot u = 0$$
$$\nabla \cdot [\eta(u)\epsilon(u) - pI] = f \qquad (2)$$

The PDE constraint in (2) is the nonlinear Stokes equations, with the nonlinearity arising from the viscosity dependence on the velocity. The viscosity $\eta(u)$ is given below in (3). It should be noted that the prefactor Γ is given in the form of an exponential to ensure that it remains positive at each iteration during an inversion.

$$\eta(u) = \Gamma \epsilon_{II}^{(1-n)/n} \qquad (3)$$

$$\Gamma = \begin{cases} e^{\mu_1}, & \Omega \\ e^{\mu_n}, & \Omega \backslash \cup_k \Omega_k \end{cases}$$

To set up the inverse problem, we need to define the Lagrangian $\mathcal{L}$ defined in (4), which is the sum of the cost functional and the weak form of (2).

$$L(u,p) = J + \int [\eta(u)\epsilon(u) : \epsilon(v) - p\nabla \cdot v - q\nabla \cdot u - f \cdot v] d\Omega \qquad (4)$$

If one takes variations with respect to the forward velocity and pressure (u,p), the forward equation (2) is obtained. However, if variations with respect to the adjoint velocity and pressure is taken, one obtains the adjoint equation in (5).

$$\nabla \cdot v = 0$$
$$\nabla \cdot [\eta(u)(I + \frac{1-n}{n}\frac{\epsilon(u)\otimes\epsilon(u)}{Tra(\epsilon(u)^2)}\epsilon(v) - qI] = 0 \qquad (5)$$

Subject to the boundary conditions given in (6), where $\hat{n}$ denotes the normal vector .

$$v \cdot n = 0$$
$$[I - \hat{n} \otimes \hat{n}][\eta(u)\left(I + \frac{1-n}{n}\frac{\epsilon(u)\otimes\epsilon(u)}{Tra(\epsilon(u)^2)}\epsilon(v) - qI\right]\boldsymbol{n} = -(u - u_d)|_{top} \qquad (6)$$

In looking at the adjoint equations in (5)-(6), one can see that the driving term is the mismatch in the surface velocities that is driving the equation as seen in (6).

Moreover, to obtain the Newton system, one will need to take the second variations of (4). Doing so, and using the Gauss-Newton approximation of the Hessian leads to the system of equations to be solve for the incremental values $\tilde{u}$, $\tilde{\Gamma}$, $\tilde{v}$ in (7).

$$\begin{bmatrix} W_{uu} & 0 & A^T \\ 0 & 0 & C^T \\ A & C & 0 \end{bmatrix} \begin{bmatrix} \tilde{u} \\ \tilde{\Gamma} \\ \tilde{v} \end{bmatrix} = - \begin{bmatrix} g_{up} \\ g_\Gamma \\ g_{vq} \end{bmatrix} \qquad (7)$$

Using Block Matrix Algebra, (7) amounts to solving (8).

$$C^T A^{-T} W_{uu} A^{-1} C\tilde{\Gamma} = -g_\Gamma$$
$$H = C^T A^{-T} W_{uu} A^{-1} C$$
$$H\tilde{\Gamma} = -g_\Gamma \qquad (8)$$

Numerical Methods

In order to invert for the weak zone values at plate boundaries, we need to solve the forward and adjoint equations given in (2) and (5). Since the forward equation is nonlinear , we would need to used Picard iteration.

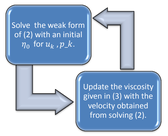

However, Picard Iteration can be slow when converging to the actual solution. Therefore, we can solve (2) by posing the problem as an optimization problem like (1). This minimization problem is given in (9).

$$\min_{u} J_2 = \int_\Omega \left(\frac{2n}{n+1}\epsilon_{II}^{\frac{n+1}{2n}} - f \cdot u \, d\Omega\right) \qquad (9)$$

As a comparison, we did a test case for a sinker for *n*=3, and the results are shown in Fig. 1, where we can see the residuals decrease faster using a Newton's method vs. Picard Iterations.

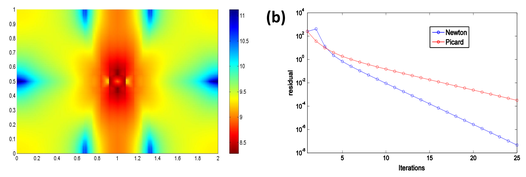

Figure 1 : (a) Eff. Viscosity for a sinker (n=3) **(b)** Residual Comparision

To solve (8), we use an inexact Newton Method with backtracking line search. This line search is the Armijo line search given below in (10).

$$d_{k+1} = d_k + \alpha_k \widetilde{d} \qquad (10)$$

Where, α_k is given below by (11).

$$\alpha_0 = 1, \rho = 0.5$$
$$\alpha_k = \rho\alpha_{k-1} \qquad (11)$$

We only accept a solution for the weak factor if the following condition in (12) is satisfied.

$$J(\Gamma_{k+1}) \leq J(\Gamma_k) + c\alpha_k g_k^T \widetilde{d_k} \qquad (12)$$

Algorithm Details

The Details of the Algorithm for the inversion of the prefactors for weak zones are given in the flow chart below.

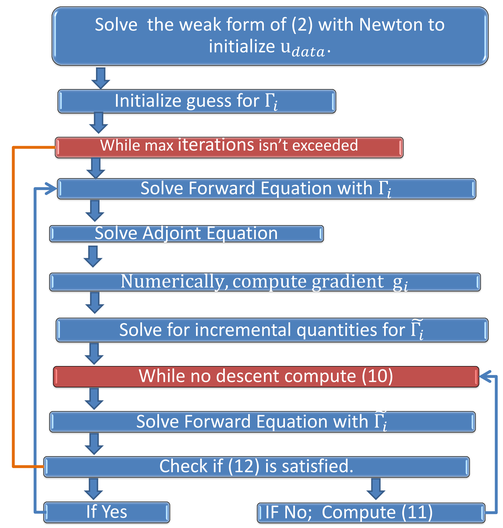

Numerical Experiments

Case I: Weak Zone with Subducting Plate

For Case I, there is a reduced viscosity zone to the left of the subducting plate, which acts essentially like a ridge as shown in Fig. 2(a). For this case we invert for the prefactor of the ridge, plate and background. We are able to recover the surface velocity Fig.2(b) almost exactly. In this case, we started with guesses of the prefactors of the slab, weak zone and background that are substantially off from the true values, but are still able to recover the exact values by iteration 14 in Fig.2(c), while driving the misfit of surface velocities in (1) to a substantially small values shown in Fig. 2(d).

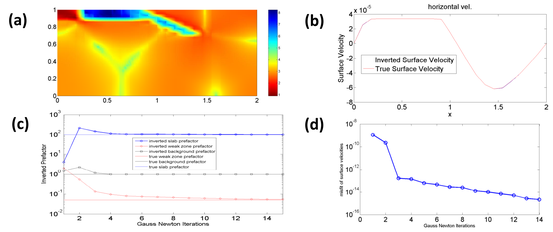

Figure 2 : (a) Eff. Viscosity **(b)** Surface Velocity Comparision **(c)** Inverted Quantities vs. Iteration **(d)**Misfit of Surface Velocities vs. Iterations.

Case II: Multiple Subducting plates and weak zones with varying pre-factors

For Case II, we look to invert for the prefactors for multiple weak zones as shown below in Fig. 3. This type of problem is one that we will be interested since it is geometrically close to the geophysical problem posed.

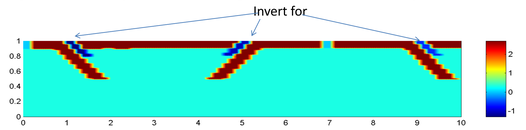

Figure 3 : Domain consisting of the prefactors defined on each stencil.

We use the algorithm presented previously to invert for the prefactor of each weakzone given in (3). It should be noted that the smallest prefactor is the weak zone on the far left while, the highest prefactor is on the far right. The effective viscosity plot is given in Fig. 4 below.

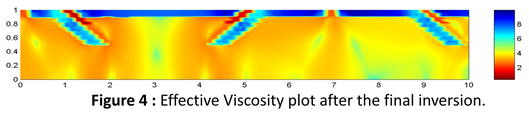

Figure 4 : Effective Viscosity plot after the final inversion.

The plot of the inverted surface velocities in comparison for the true surface which shows we are able to essentially recover the exact surface velocity as shown in Fig. 5.

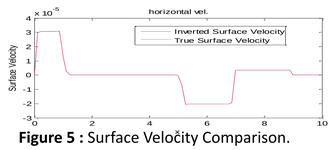

Figure 5 : Surface Velocity Comparison.

In Fig. 6, we are able to recover the true prefactors for each weak zone almost exactly by 2 Gauss-Newton Iterations.

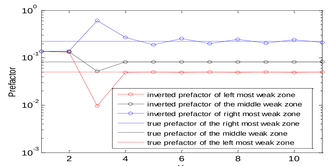

Figure 6 : Prefactor Inversion vs. Iterations

In Fig. 7, we are able drive the misfit of surface velocities defined in (1) to significantly small values.

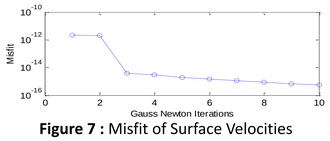

Figure 7 : Misfit of Surface Velocities

Next Steps

We have developed a robust and scalable method to invert for the prefactor of the weak zone. The next phase would be to apply this methodology to global models with realistic temperature fields etc. as shown in Fig. 8.

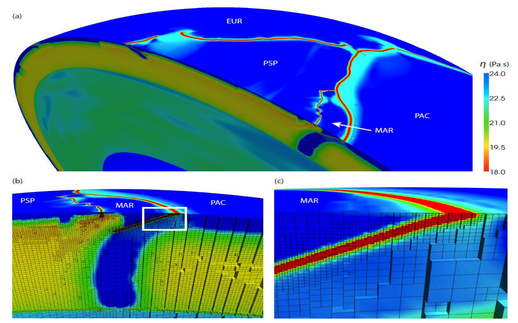

Figure 8 : Example of global models with fine scale resolution that will be used for inversion taken from Alisic et. al.(2012)

An example of how varying parameters in the rheological law can lead to mismatches in surface velocity is shown in Fig. 9 below. By inverting for the values of the weak zones where we minimize the mismatch in said surface velocities, we can achieve a better fitting model with the properly constrained surface velocities.

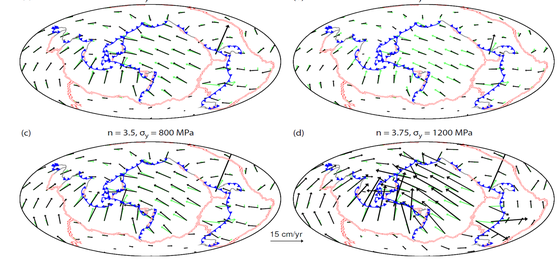

Figure 9: Example of the misfit of surface velocities for global models for various perturbations of rheological parameters taken from Alisic et. al.(2012)

Additionally, we will look at regional models like the ones shown below in Fig. 10 where there is better data coverage in order for the quality of the inversion is better due to more information being available in certain regions.

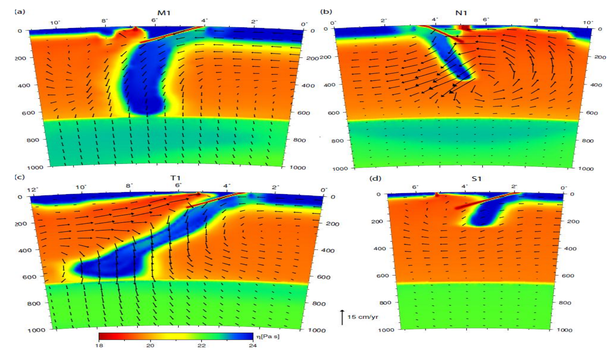

Figure 10: Various Regional models with their corresponding effective viscosity and velocity fields, taken from Alisic et. al.(2012)

Future Directions

- **Forthcoming investigations will use a non-Newtonian rheology with yielding that is widely used for mantle convection problems.**
- **Investigate adding noise to the plate velocities to test the limits of how well we can recover the strength of the weak zones.**
- **Apply these inverse methods to global plate motions and infer the strength of plate coupling at convergent plate boundaries.**